

The relative importance of ejections and sweeps to momentum transfer in the atmospheric boundary layer

Gabriel Katul · Davide Poggi · Daniela Cava · John Finnigan

Received: 9 June 2005 / Accepted: 8 December 2005
© Springer Science+Business Media B.V. 2006

Abstract Using an incomplete third-order cumulant expansion method (ICEM) and standard second-order closure principles, we show that the imbalance in the stress contribution of sweeps and ejections to momentum transfer (ΔS_o) can be predicted from measured profiles of the Reynolds stress and the longitudinal velocity standard deviation for different boundary-layer regions. The ICEM approximation is independently verified using flume data, atmospheric surface layer measurements above grass and ice-sheet surfaces, and within the canopy sublayer of maturing Loblolly pine and alpine hardwood forests. The model skill for discriminating whether sweeps or ejections dominate momentum transfer (e.g. the sign of ΔS_o) agrees well with wind-tunnel measurements in the outer and surface layers, and flume measurements within the canopy sublayer for both sparse and dense vegetation. The broader impact of this work is that the “genesis” of the imbalance in ΔS_o is primarily governed by how boundary conditions impact first and second moments.

G. Katul (✉) · D. Poggi
Nicholas School of the Environment and Earth Sciences,
Duke University Box 90328, Durham, NC, USA
e-mail: gaby@duke.edu

G. Katul
Department of Civil and Environmental Engineering,
Duke University, Durham, NC, USA

D. Poggi
Dipartimento di Idraulica Trasporti e Infrastrutture Civili, Politecnico di Torino,
Corso Duca degli Abruzzi, 24
10129, Torino, Italy

D. Cava
CNR - Institute of Atmospheric Sciences and Climate, Section of Lecce,
Polo Scientifico dell'Università
Strada Prov. Lecce-Monteroni km 1,200
73100 Lecce, Italy

J. Finnigan
CSIRO Marine and Atmospheric Research, FC Pye Laboratory, Black Mountain,
Canberra, ACT 2601, Australia

Keywords Canopy turbulence · Closure modelling · Cumulant expansions · Ejections and sweeps · Momentum transfer

1. Introduction

The interest in ejections and sweeps dates back to early experiments by Kline et al. (1967) who demonstrated via flow visualization that fluid motion near a wall is “*far from being completely chaotic in nature*” revealing a definite “*sequence of ordered motion*”. To quantify the impact on momentum transfer of such coherent motion, often called the bursting or ejection-sweep cycle, several techniques were proposed and tested (Robinson 1991). A popular technique, known as conditional sampling and quadrant analysis, was introduced by Lu and Willmarth (1973) to detect signatures of such coherent motion in component velocity time series and to derive quantitative information about them (see reviews in Antonia 1981; also Cantwell 1981). Building on earlier work by Frenkiel and Klebanoff (1967), Nakagawa and Nezu (1977) and Raupach (1981) employed a two-dimensional Gram-Charlier cumulant expansion method (CEM) for the joint probability density function (JPDF) of turbulent longitudinal (u') and vertical (w') velocity components to link non-Gaussian JPDF with the statistical properties of the ejection-sweep cycle. In particular, the CEM approach used by Nakagawa and Nezu (1977) was able to analytically couple the imbalance in stress contribution of sweeps and ejections to turbulent diffusion processes through the third (or mixed) moments. Such a linkage was timely because advances in second-order closure modelling required better parameterization of the turbulent diffusion processes (Hanjalic and Launder 1972; Mellor 1973; Donaldson 1973; Lumley 1978). Hence, it is no surprise that the imbalance in the stress contribution of sweeps and ejections and non-Gaussian JPDF received significant experimental and theoretical attention (e.g. Durst et al. 1992; Jovanovic et al. 1993; Durst and Jovanovic 1995).

Within the atmospheric boundary layer (ABL), the asymmetry in the JPDF also motivated model developments such as top-down/ bottom-up diffusion (e.g. Weil 1990; Sorbjan 1999; Patton et al. 2003) or structural models for the triple moments that require a priori knowledge as to whether sweeps or ejections dominate the momentum transfer (Nagano and Tagawa 1990).

Here, we investigate whether the profiles of first and second moments in the ABL are sufficient to predict a priori whether ejections or sweeps dominate momentum transfer. If successful, the implication of this work is that the “genesis” of this imbalance can be explained by how boundary conditions impact lower-order moments.

2. Theory

The ejection-sweep cycle is typically quantified via quadrant analysis and conditional sampling methods reviewed in Antonia (1981). Quadrant analysis refers to the joint scatter across four quadrants defined by a Cartesian plane whose abscissa is u' and ordinate is w' . The four quadrants are connected with four modes of momentum transfer: events in quadrant II ($u' < 0$, $w' > 0$) and quadrant IV ($u' > 0$ and $w' < 0$) are called ejections and sweeps respectively; events in quadrant I ($u' > 0$ and $w' > 0$) and quadrant III ($u' < 0$ and $w' < 0$) are called outward and inward interactions, respectively.

Nakagawa and Nezu (1977) and Raupach (1981) defined the imbalance in the contribution of sweeps and ejections to momentum transfer using the difference in stress fraction contributions of quadrant II and quadrant IV:

$$\Delta S_o = \frac{\overline{u'w'}_{IV} - \overline{u'w'}_{II}}{\overline{u'w'}} \tag{1}$$

where $\overline{u'w'}$ is the momentum flux and $\frac{\overline{u'w'}_{IV}}{\overline{u'w'}}$ and $\frac{\overline{u'w'}_{II}}{\overline{u'w'}}$ are the stress fractions in quadrants IV and II, respectively. The definition in Eq. (1) ensures that ΔS_o is bounded between -1 and 1 (assuming $|\overline{u'w'}| > 0$). Based on this definition, sweeps dominate the momentum transfer when $\Delta S_o > 0$, and conversely. Because ΔS_o becomes ill-defined when $|\overline{u'w'}| \rightarrow 0$, our analysis is restricted to cases when $|\overline{u'w'}|$ is finite. This restriction implies that the purely convective boundary layer will not be treated here.

Using the Gram-Charlier series expansion of the JPFD (Kampé de Fèriet 1966), truncated to the third order, Raupach (1981) demonstrated that

$$\Delta S_o = \frac{1 + R_{uw}}{R_{uw}\sqrt{2\pi}} \left[\frac{2C_1}{(1 + R_{uw})^2} + \frac{C_2}{1 + R_{uw}} \right] \tag{2}$$

where,

$$C_1 = (1 + R_{uw}) \left[\frac{1}{6} (M_{03} - M_{30}) + \frac{1}{2} (M_{12} - M_{21}) \right],$$

$$C_2 = - \left[\frac{1}{6} (2 - R_{uw}) (M_{03} - M_{30}) + \frac{1}{2} (M_{12} - M_{21}) \right],$$

and $R_{uw} = \frac{\overline{u'w'}}{\sigma_u \sigma_w}$, $M_{ji} = \frac{\overline{u'^j w'^i}}{\sigma_u^j \sigma_w^i}$, $\sigma_s = \sqrt{s'^2}$ and where $u'^j|_{j=2} \rightarrow u'^2$, etc. . .

Katul et al. (1997a, b) noted that for the range of skewness values encountered in the atmospheric boundary layer (including canopy turbulence), the contribution of the $\frac{1}{6} (M_{03} - M_{30})$ to Eq. (2) is small, which lead Katul et al. (1997a, b) to further simplify Eq. (2) to give:

$$\Delta S_o \approx \frac{1}{2R_{uw}\sqrt{2\pi}} (M_{21} - M_{12}) \tag{3}$$

where,

$$M_{21} = \frac{\overline{w'u'u'}}{\sigma_w \sigma_u^2}, \tag{4a}$$

$$M_{12} = \frac{\overline{w'w'u'}}{\sigma_u \sigma_w^2}. \tag{4b}$$

We refer to Eq. (3) as an incomplete cumulant expansion (ICEM) because of the elimination of the velocity skewness.

We tested predictions from Eq. (3) against quadrant analysis using laboratory and field measurements collected over a wide range of atmospheric conditions (Fig. 1). The flume data are collected within and above a dense canopy composed of cylindrical rods (Poggi et al. 2004a, b); the field datasets include surface-layer measurements above tall grass (Katul et al. 1997a) and ice surfaces (Cava et al. 2001, 2005); and the forest canopy data include measurements within a maturing pine stand (Katul and Albertson 1998) and an alpine hardwood forest (Cava et al. 2006). The measurements within the Antarctic surface layer above ice also include runs sampled at different heights for planar homogeneous flows, flows perturbed by katabatic winds, and flows perturbed by a ridge. When taken together, this ensemble dataset populates the entire plausible values of ΔS_o (i.e. -1 to 1) as shown in Figure 1.

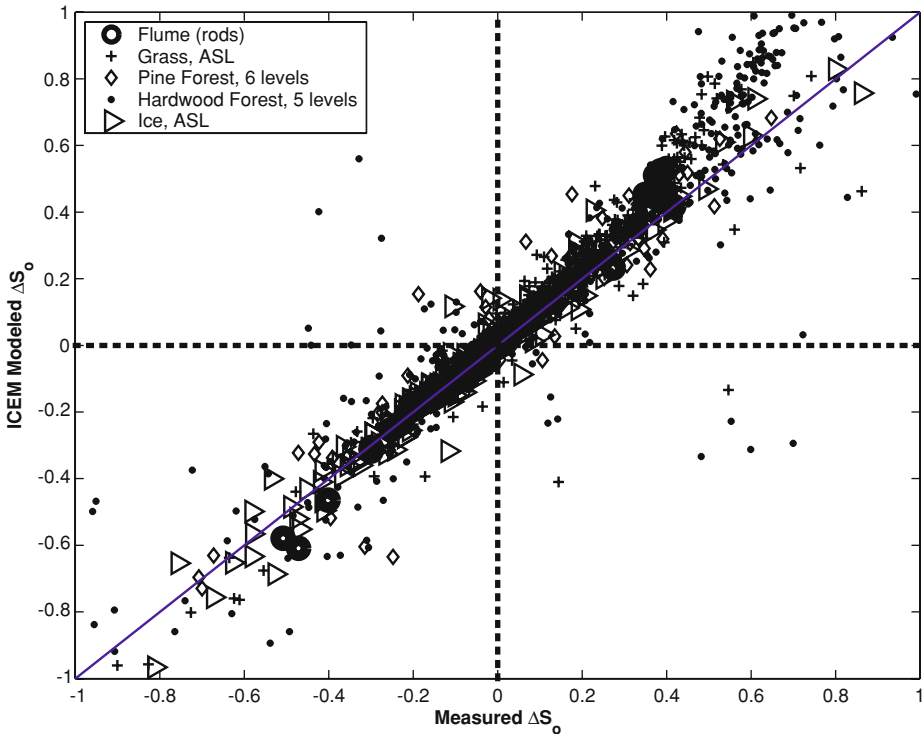


Fig. 1 Comparison between measured (i.e. quadrant analysis) and ICEM modelled ΔS_o . The open circles are from a flume experiment comprised of cylindrical rods (dense canopy); the diamonds are data taken from six levels within a maturing Loblolly pine forest; the stars are data from a surface-layer experiment above a tall grass surface; the diamond are data taken from five levels within an alpine hardwood forest; and the triangles are data taken in an Antarctic surface layer and include runs in which the surface layer is perturbed by the presence of a ridge. The field experiments include a wide range of atmospheric stability conditions. The 1:1 line is shown for reference. Regressing the modelled ($\hat{y} = \text{ICEM}$) upon the measured ($\hat{x} = \text{quadrant analysis}$) ΔS_o using all the data ($n = 1340$ points) yields $\hat{y} = 1.0\hat{x} + 0.031$ with a coefficient of determination $R^2 = 0.92$

Despite the simplifications in its derivation (i.e. truncation of cumulants beyond order 3 and elimination of the two velocity skewness values), Eq. (3) reproduces the measured ΔS_o surprisingly well ($R^2 = 0.92$, regression slope = 1.0, regression intercept = 0.03; sample size $n = 1,341$). In addition to the comparisons in Fig. 1, Eq. (3) was independently tested by Katul et al. (1997a) in the atmospheric surface layer above a bare soil surface for a wide range of stability conditions, Katul et al. (1997b) near the canopy top of a maturing pine forest and a southern hardwood canopy also for a wide range of atmospheric stability conditions, and more recently by Fer et al. (2004) for under-ice boundary-layer flows. All three studies reported $R^2 > 0.9$ in their comparisons.

Next, we consider whether Eq. (3) can be used to link ΔS_o to second-order flow statistics thereby addressing the study objectives. Upon replacing the moments in Eq. (4) back into Eq. (3), we obtain

$$\Delta S_o \approx \frac{1}{2\sqrt{2\pi} \overline{u'w'}} \left(\frac{\overline{w'u'u'}}{\sigma_u} - \frac{\overline{w'w'u'}}{\sigma_w} \right). \quad (5)$$

Standard gradient-diffusion closure for the triple moments results in (e.g. Wilson and Shaw 1977):

$$\overline{u'_i u'_j u'_k} = -q\lambda \left(\frac{d\overline{u'_j u'_k}}{dx_i} + \frac{d\overline{u'_i u'_k}}{dx_j} + \frac{d\overline{u'_i u'_j}}{dx_k} \right)$$

where $q = \sqrt{\overline{u'u'} + \overline{v'v'} + \overline{w'w'}}$ is a characteristic turbulent velocity and λ is an unknown characteristic length for the triple moments. For a one-dimensional case, $\overline{w'u'u'}$ and $\overline{w'u'w'}$ are given by

$$\overline{w'u'u'} = -q\lambda \frac{d\overline{u'u'}}{dz}, \quad (6a)$$

$$\overline{w'u'w'} = -2q\lambda \frac{d\overline{u'w'}}{dz}. \quad (6b)$$

Upon combining Equations (6) and (5), we obtain (Poggi et al. 2004b)

$$\Delta S_o \approx \frac{-q\lambda}{2\overline{u'w'}\sqrt{2\pi}} \left(\frac{1}{\sigma_u} \frac{d\sigma_u^2}{dz} - \frac{2}{\sigma_w} \frac{d\overline{u'w'}}{dz} \right). \quad (7)$$

Again, it is not our intention to investigate the magnitudes of ΔS_o predicted by Eq. (7) because such an investigation requires a rigorous determination of λ in Eq. (6) and accurate measurements of the profiles of the second-order moments. However, Eq. (7) does offer a desirable predictive skill: the sign of ΔS_o . That is, solely from the relative importance of the profiles of second-order statistics, it is possible to distinguish whether momentum transfer will be dominated by sweeps or ejections, the objective of this study.

3. Results and discussion

We consider next all three layers of the ABL: the outer region, the dynamic sub-layer, and the canopy sublayer (sparse and dense), and we evaluate whether changes in $\frac{d\sigma_u}{dz}$ and $\frac{d\overline{u'w'}}{dz}$ explain the sign of ΔS_o (measured by quadrant analysis). For the purposes of the following discussion, we introduce four length scales: z —the height from the ground surface, d —the zero-displacement height, h —the canopy height, δ —the ABL height and consider the four cases below.

Case (1)—The Outer Region. In the outer region, roughly the region defined by $\frac{(z-d)}{\delta} > 0.4$, Raupach's (1981) wind-tunnel experiments suggest that $\overline{u'w'} < 0$, $\frac{d\sigma_u^2}{dz} < 0$, and $\frac{d\overline{u'w'}}{dz} > 0$ for both rough and smooth boundary layers (Fig. 2). Based on the sign of these three quantities in Fig. 2, Eq. (7) unambiguously predicts $\Delta S_o < 0$ (i.e. ejections dominate) consistent with the measured ΔS_o by quadrant analysis.

Case (2)—The constant stress layer. In the neutral atmospheric surface layer (or dynamic sublayer), defined as the constant stress region (see region bounded by $0.1 < \frac{(z-d)}{\delta} < 0.2$ in Fig. 2), surface-layer similarity theory predicts that $\frac{\sigma_u}{u_*} \approx 2.0$; $\frac{\overline{u'w'}}{u_*^2} = -1$, $\frac{d\sigma_u^2}{dz} = 0$, $\frac{d\overline{u'w'}}{dz} = 0$ and via Eq. (7), $\Delta S_o = 0$ also in agreement with the measurements (Fig. 2).

The fact that ejections and sweeps equally contribute to momentum transfer is also in agreement with other surface-layer measurements above grass and bare soil surfaces (Katul

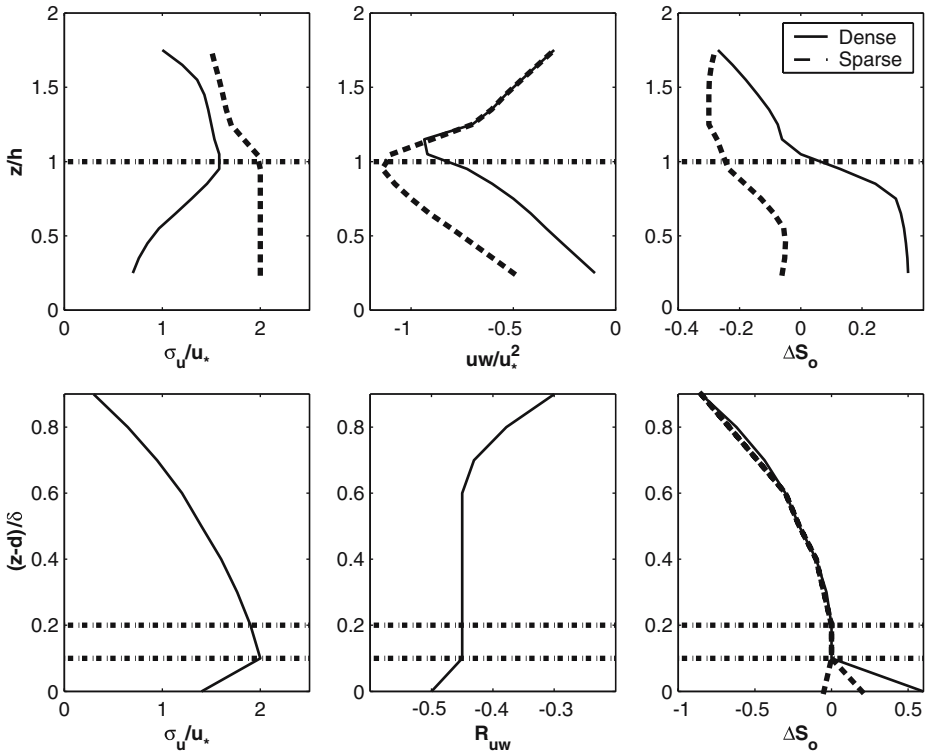


Fig. 2 Measured σ_u , Reynolds stress ($\overline{u'w'}$ or R_{uw}), and ΔS_o profiles within the canopy sublayer (top), and within the constant stress and outer layers of the neutral ABL. For the canopy sublayer, data are collected in a flume for sparse (dashed) and dense (solid) canopies (Poggi et al., 2004a). For the surface and outer layers, data are collected in a boundary-layer wind tunnel for rough and smooth surfaces (Raupach 1981). The lines in the bottom right ΔS_o panel are for various roughness values in Raupach (1981)

et al. 1997a; $|\frac{z-d}{L}| < 0.05$ and $z/h > 4$, where L is the Obukhov length). Furthermore, this conclusion is consistent with several atmospheric surface-layer experiments that already reported the JPDF to be approximately Gaussian for the surface layer (e.g. Chu et al. 1996).

Case (3)—The canopy sublayer inside sparse canopies. From Poggi et al.'s (2004a) flume experiments, a near constant σ_u and σ_w , but an increasing $\overline{u'w'}$ (i.e. less negative) with increasing z , were measured inside sparse canopies (see $z/h < 1$ in Fig. 2). For constant σ_u and σ_w and $\frac{d\overline{u'w'}}{dz} > 0$, Eq. (7) unambiguously predicts that ejections must dominate momentum transfer for such conditions consistent with the ΔS_o data in Fig. 2.

Case (4)—The canopy sublayer inside dense canopies. All three variables, $\frac{d\sigma_u}{dz}$, $\frac{d\sigma_w}{dz}$, and $-\frac{d\overline{u'w'}}{dz}$ vary significantly within the canopy (see $z/h < 1$ in Fig. 2). However, all three gradients are known to be positive (i.e. $\frac{d\sigma_u}{dz} > 0$, $\frac{d\sigma_w}{dz} > 0$, and $-\frac{d\overline{u'w'}}{dz} > 0$) as evidenced from laboratory and field experiments (see review in Finnigan 2000) and the data in Fig. 2. When we combine this sign outcome with Eq. (7), the sign of ΔS_o must be controlled by $-\overline{u'w'}$. If $\overline{u'w'} < 0$, $\Delta S_o > 0$ and sweeps dominate the momentum transfer. The fact that sweeps dominate momentum transfer was already reported in numerous laboratory and flume experiments (see Finnigan 2000; Poggi et al. 2004a,b), field experiments (e.g. Shaw

et al. 1983 for corn; Baldocchi and Meyers 1988 for a hardwood forest; Katul and Albertson 1998 for a pine forest), and large-eddy simulations¹ (Su et al. 1998).

However, one surprise from Eq. (7) is the case when $\overline{u'w'} > 0$ (which is possible inside canopies as evidenced by the data in Katul and Albertson 1998 and Baldocchi and Meyers 1988). For this condition, Eq. (7) predicts that $\Delta S_o < 0$ and ejections dominate the momentum transfer. We caution that the latter prediction may well be questionable primarily because of the gradient-diffusion approximation in Eq. (6) (rather than the ICEM approximation).

3.1. Robustness to gradient-diffusion approximations

We note that predictions by Eq. (7) may be more robust to the gradient-diffusion approximation when compared to Eq. (6). To illustrate, consider the extensive surface-layer dataset in Kader and Yaglom (1990). A finite $\overline{w'u'w'}$ was reported for the near-neutral surface layer despite their constant friction velocity (u_*). Equation (6) would predict $\overline{w'u'w'} = 0$ if $d\overline{u'w'}/dz = 0$. Hence, based on this argument alone, predictions from Eq. (7) may well be contaminated by a non-trivial error. Let us assess how such ‘gross’ errors in Eq. (6) might affect predictions from Eq. (7).

Kader and Yaglom (1990) do not report $\overline{w'u'u'}$ and hence we cannot fully test Eq. (7) for velocity. However, they do report analogous moments for air temperature (T). If we use Kader and Yaglom’s (1990) data for temperature, we find the following for the near-neutral surface layer:

$$\frac{\overline{w'w'T'}}{u_*^2 T_*} = 0.55; \quad \frac{\overline{w'T'T'}}{u_* T_*^2} = 1.2; \quad \frac{\sigma_T}{T_*} = 2.9; \quad \frac{\sigma_w}{u_*} = 1.25.$$

With these estimates

$$M_{21} = \frac{\overline{w'T'T'}}{\sigma_w \sigma_T^2} = \left(\frac{1.2}{1.25 (2.9)^2} \right) \left(\frac{u_* T_*^2}{u_* T_*^2} \right) = 0.11,$$

$$M_{12} = \frac{\overline{w'w'T'}}{\sigma_w^2 \sigma_T} = \left(\frac{0.55}{(1.25)^2 2.9} \right) \left(\frac{u_*^2 T_*}{u_*^2 T_*} \right) \approx 0.12,$$

resulting in

$$\Delta S_o \approx \frac{1}{2R_{wT}\sqrt{2\pi}} (M_{21} - M_{12}) \approx 0$$

if R_{wT} is finite (or non-zero sensible heat flux). Hence, for near-neutral surface-layer flows, the Kader and Yaglom (1990) data would have yielded $\Delta S_o \approx 0$ assuming the ICEM expansion, tested in Fig. 1, is accurate at their station. Gradient-diffusion argument (Eq. 5) would have erroneously predicted that $M_{12} \approx M_{21} \approx 0$, but Eq. (7) would have correctly predicted that sweeps and ejections are in balance. Interestingly, what is important here is to model correctly *not* the individual moments but the imbalance between them.

¹ While the authors state that their canopy is sparse, the inflection point in their mean velocity profile appears sufficient to induce Kelvin-Helmholtz instabilities, at least when compared to the sparse canopy in the flume experiments of Poggi et al. (2004a).

4. Conclusions

We have demonstrated that the incomplete third-order cumulant expansion (ICEM) approach reproduces the sign and magnitude of ΔS_o surprisingly well, and that when combined with standard second-order closure principles, can analytically link ΔS_o to the profiles of $\frac{d\sigma_u}{dz}$, $\frac{d\sigma_w}{dz}$, and $-\frac{d\overline{u'w'}}{dz}$. Using this linkage, we showed that in the:

- 1) outer layer, $\Delta S_o < 0$ and ejections dominate momentum transfer;
- 2) neutral surface layer, $\Delta S_o = 0$ and a balance between ejections and sweeps exists;
- 3) sparse canopy sublayer, $\Delta S_o < 0$ and ejections dominate momentum transfer;
- 4) dense canopy sublayer, $\Delta S_o > 0$ and sweeps dominate momentum transfer through out most of the canopy.

None of these four findings is particularly new; however, the ability to predict them from the profiles of σ_u^2 , σ_w^2 , and $\overline{u'w'}$ is one of the main novelties of this work. The broader impact of our findings can be summarized as follows. If ΔS_o does capture the statistical properties of the ejection–sweep cycle, then these properties are a “by-product” of how the boundary conditions produce non-uniformity in the first- and second-order velocity statistics. Within the canopy sublayer, the critical boundary condition is the fact that the drag of the canopy on the flow is extended in the vertical rather than being confined to the ground plane; within the outer layer, the critical boundary condition is the decay of turbulence near the ABL top; and within the surface layer, the critical condition is the balance between the control of the dynamics by the upper and lower boundary conditions (Kader and Yaglom 1978).

While the approach proposed in Eq. (7) was successful in predicting the sign of ΔS_o for flat terrain under steady-state neutral conditions, several problems remain. For example, whether this model can predict the local sign of ΔS_o in the presence of strong mean pressure gradients (e.g. topography induced), or when a horizontal heterogeneity length scale (e.g. forest edges) dominates the advective transport, remains to be investigated. Nonetheless, this approach provides a simplified framework with which to confront these complex issues.

Acknowledgements The first author acknowledges support from the National Science Foundation (NSF-EAR and NSF-DMS), the Biological and Environmental Research (BER) Program, US Department of Energy, through the south-east Regional Center (SERC) of the National Institute for Global Environmental Change (NIGEC), and through the Terrestrial Carbon Processes Program (TCP). D. Cava acknowledges the Italian National Program for Research in Antarctica (PNRA). D. Poggi acknowledges support from COFIN - Programmi di Ricerca Scientifica di Rilevante Interesse Nazionale (PRIN P rot. 2002087584-008).

References

- Antonia RA (1981) Conditional sampling in turbulence measurements. *Ann Rev Fluid Mech* 13:131–156
- Baldocchi D, Meyers TP (1988) Turbulence structure in a deciduous forest. *Boundary-Layer Meteorol* 43: 345–364
- Cantwell B (1981) Organized motion in turbulent flow. *Ann Rev Fluid Mech* 13:457–515
- Cava D, Giostra U, Tagliazuca M (2001) Spectral maxima in a perturbed atmospheric boundary layer. *Boundary-Layer Meteorol.* 100:421–437
- Cava D, Schipa S, Giostra U (2005) Investigation of low-frequency perturbations induced by a steep obstacle. *Boundary-Layer Meteorol* 115:27–45
- Cava D, Katul GG, Scrimieri A, Poggi D, Cescatti A, Giostra U (2006) Buoyancy and the sensible heat flux budget within dense canopies. *Boundary-Layer Meteorol* 118:217–240
- Chu CR, Parlange MB, Katul GG, Albertson JD (1996) Probability density functions of turbulent velocity and temperature in the atmospheric surface layer. *Water Resour Res* 32:1681–1688

- Donaldson C Du P (1973) Construction of a dynamic model for the production of atmospheric turbulence and the dispersion of atmospheric pollutants. In Workshop on Micrometeorology, American Meteorological Society, 45 Beacon St., Boston, MA, pp. 313–392
- Durst F, Jovanovic J, Johansson TG (1992) On the statistical proprieties of truncated gram-Charlier series expansions in turbulent wall-bounded flows. *Phys Fluids A* 4(1):118–126
- Durst F, Jovanovic (1995) Investigations of Reynolds-Averaged turbulence quantities. *Proc Roy Soc A* 451 (1941):105–120
- Fer I, McPhee MG, Sirevaag A (2004) Conditional statistics of the Reynolds stress in the under-ice boundary layer. *Geophys Res Lett* 31:2004GL020475
- Finnigan J (2000) Turbulence in plant canopies. *Ann Rev Fluid Mech* 32:519–571
- Frenkiel F, Klebanoff P (1967) Higher order correlations in a turbulent field. *Phys Fluids* 10:507–522
- Hanjalic K, Launder BE (1972) A Reynolds stress model for turbulence and its application to thin shear flows. *J Fluid Mech* 52:609–638
- Jovanovic J, Durst F, Johansson TG (1993) Statistical analysis of the dynamic equations for higher-order moments in turbulent wall bounded flows. *Phys Fluids A* 5(11):2886–2900
- Kader BA, Yaglom AM (1978) Similarity treatment of moving-equilibrium turbulent boundary layers in adverse pressure-gradients. *J Fluid Mech* 89:305–342
- Kader BA, Yaglom AM, (1990) Mean fields and fluctuation moments in unstably stratified turbulent boundary layers. *J Fluid Mech* 212:637–662
- Kampé de Fériet J (1966) The Gram-Charlier approximation of the normal law and the statistical description of a homogeneous turbulent flow near statistical equilibrium. Model Basin Report No. 2013, Naval Ship Research and Development Center, Washington, DC, 1966
- Katul GG, Kuhn G, Scheildge J, Hsieh CI, (1997a) The ejection-sweep character of scalar fluxes in the unstable surface layer. *Boundary-Layer Meteorol* 83:1–26
- Katul GG, Hsieh CI, Kuhn G, Ellsworth D, Nie D (1997b) Turbulent eddy motion at the forest-atmosphere interface. *J. Geophys Res* 102:13409–13421
- Katul GG, Albertson JD, (1998) An investigation of higher order closure models for a forested canopy. *Boundary-Layer Meteorol* 89:47–74
- Kline SJ, Reynolds WC, Schraub FA, Runstadler PW (1967) The structure of turbulent boundary layers. *J. Fluid Mech* 30:741–773
- Lu SS, Willmarth WW (1973) Measurements of the structure of Reynolds stress in a turbulent boundary layer. *J Fluid Mech* 60:481–571
- Lumley JL (1978) Computational modelling of turbulent flows. *Adv Appl Mech* 18:123
- Mellor G (1973) Analytic prediction of the properties of stratified planetary boundary layer. *J Atmos Sci* 30:1061–1069
- Nagano Y, Tagawa M, (1990) A structural turbulence model for triple products of velocity and scalar. *J Fluid Mech* 196:157–185
- Nakagawa H, Nezu I (1977) Prediction of the contributions to the Reynolds stress from bursting events in open channel flows. *J Fluid Mech* 80:99–128
- Patton N, Sullivan PP, Davis KJ (2003) The influence of a forest canopy on top-down and bottom-up diffusion in the planetary boundary layer. *Quart J Roy Meteorol Soc* 129: 1415–1434
- Poggi D, Porporato A, Ridolfi L, Albertson JD, Katul GG, (2004a) The effect of vegetation density on canopy sub-layer turbulence. *Boundary-Layer Meteorol* 111:565–587
- Poggi D, Katul GG, Albertson JD (2004b) Momentum transfer and turbulent kinetic energy budgets within a dense model canopy. *Boundary-Layer Meteorol* 111:589–614
- Raupach MR (1981) Conditional statistics of Reynolds stress in rough-wall and smooth-wall turbulent boundary layers. *J Fluid Mech* 108:363–382
- Robinson SK (1991) Coherent motions in the turbulent boundary layer. *Ann Rev Fluid Mech* 23:601–639
- Shaw RH, Tavangar J, Ward D (1983) Structure of the Reynolds stress in a canopy layer. *J Clim Appl Meteorol* 22:1922–1931
- Su HB, Shaw RH, Paw U, K.T., Moeng CH, Sullivan P (1998) Turbulent statistics of neutrally stratified flow within and above a sparse forest from Large-Eddy Simulation and field observations. *Boundary-Layer Meteorol* 88:363–397
- Sorbjan Z (1999) Similarity of scalar fields in the convective boundary layer. *J Atmos Sci* 56:2212–2221
- Weil JC (1990) A diagnosis of the asymmetry in top-down and bottom-up diffusion using a Lagrangian stochastic model. *J Atmos Sci* 47:501–515
- Wilson NR, Shaw RH (1977) A higher order closure model for canopy flow. *J Appl Meteorol* 16:1198–1205